steel research international
www.steel-research.de



# Multi-Response Optimization of the Thermal and Thermomechanical Behavior of a Steel Ladle Lining using Grey Relational Analysis and Technique for Order Preference by Similarity to Ideal Solution

*Aidong Hou,* Dietmar Gruber, and Shengli Jin*

**The present research attempts to simultaneously optimize the thermal and thermomechanical behavior of a steel ladle lining. The lining configurations are designed with an L32 orthogonal array considering the input parameters of various material properties and lining thicknesses. From the finite-element (FE) simulations, three responses are evaluated: the end temperature and maximum tensile stress at the steel shell and the maximum compressive stress at the hot face of the working lining. Multi-response optimization is performed through grey relational analysis (GRA) and the technique for order preference by similarity to ideal solution (TOPSIS) by applying a distinguishing coefficient of 0.5 in GRA and the signal-to-noise (S/N) ratio-based weight in both techniques. Both GRA and TOPSIS results yield the same best solution (the fourth lining configuration) and the same optimal levels for significant factors. Analysis of variance (ANOVA) is used to identify the significance of the factors and their contributions to the overall performance characteristic. The results demonstrate that the top five factors with the analyses of GRA and TOPSIS are the same and their total contribution is similar.**

## 1. Introduction

Steel ladles, constructed with refractories and steel components, play a crucial role in secondary steelmaking metallurgy. They act as transfer and refining vessels for molten steel and are exposed to a harsh operating environment during service.[1,2] Therefore, a well-designed steel ladle increases its lifetime, steel quality, and productivity, favors environment-friendly missions, and reduces energy consumption and refractory costs.[1,2]

The design and optimization of a steel ladle lining is a complex process because the thermal and thermomechanical performance of a lining is affected by several factors, such as process conditions[3–7] and lining configurations,[8–15] for instance, presence or absence of an insulation, lining thicknesses, material selection, and joints. Significant efforts have been devoted toward facilitating the design and optimization of steel ladle linings. Previous studies[3–5] revealed that using ladles without preheating may lead to the compressive failure of the working lining owing to the high compressive stresses on the hot face. These stresses can be reduced by a 15–20 h preheating;[6] a 30 min preheating during the empty ladle process can raise the average temperature of the working lining by 130.3 K and reduce the molten steel temperature drop rate by 0.11 K min$^{-1}$ compared to a case without preheating.[7] The application of an insulating layer between the permanent lining and the steel shell has a significant influence on the performance of the ladle.[4,8–10] In contrast, the presence of the insulating layer can reduce heat loss and lower shell temperatures. However, it may cause higher operating temperatures[9] and higher irreversible strains[4] in the inner refractory linings, reducing the lifetime of the lining. A study by Santos et al.[9] revealed that working lining materials with lower thermal conductivities exhibited excellent performance in saving energy and reducing average shell temperatures. The application of a C-free working layer can reduce the tapping temperature by 16 °C and energy consumption by 20% because of the hindered heat transfer due to the lack of carbon and the presence of lower thermal conductivity phases, for instance, microporous phases.[11] Homogenized numerical models were developed by Ali et al.[12,13] to simulate the transient thermomechanical behavior during a typical steel–ladle thermal cycle. The working lining and bottom of the ladle were replaced with an equivalent material model that considered the presence of dry joints and their closure and reopening under cyclic thermal or mechanical loading/unloading. The results demonstrated that the behavior of mortarless masonry is orthotropic and nonlinear owing to joint closure and reopening, and the thermal stresses in the wall of the working lining, bottom, and steel shell decreased with increasing joint thickness. A decreased

A. Hou, D. Gruber, S. Jin
Chair of Ceramics
Montanuniversitaet Leoben
A-8700 Leoben, Austria
E-mail: aidong.hou@unileoben.ac.at

The ORCID identification number(s) for the author(s) of this article can be found under https://doi.org/10.1002/srin.202200407.



**DOI: 10.1002/srin.202200407**

maximum von Mises stress in the steel shell was obtained when the bricks at the bottom were arranged with the longer edge in the circumferential direction of the cylinder and the mortar joints were 3 mm.[14] Li et al.[15] proposed the use of at least 2 mm axial expansion joints of the ladle bottom to reduce the contact stresses between the working and permanent layers.

Previous studies mainly focused on the influence of one or two factors and the quantitative significance of the factors for responses has not been reported. However, steel ladle lining optimization from the thermal and thermomechanical perspective is a multi-objective optimization problem. Therefore, a methodology that provides holistic design and quantitative information is required. Santos et al.[16] proposed an evolutionary screening procedure (ESP) for the material selection of furnace linings and applied it to an electric resistance furnace. ESP is a systematic selection methodology based on a quantitative strategy, whereby furnace designers can save time and visualize scenarios with more reliable information. Exploration of variable codes was developed in the framework of the integration variable method by Asgher et al.[17] for the material selection of a metallurgical ladle based on system constraints. Santos and Asgher aimed to obtain a lining configuration with a low total lining thickness, material costs, and external temperature; however, thermomechanical performance was not considered. In a previous study,[18] the authors introduced a single objective optimization technique, the Taguchi method, to optimize the thermal and thermomechanical behavior of a ladle lining. The Taguchi method offered the optimal solution and the percentage of factor contribution for each response; however, it is not suitable for optimizing the multiple responses simultaneously. When some factors have a contradictory impact on different responses, it poses a challenge when making trade-off decisions. For instance, thicker insulation results in lower steel shell temperatures and higher tensile stresses on the steel shell. In this case, expert experience is required to inform the decisions.

The present study aims to simultaneously optimize the thermal and thermomechanical behavior of a steel ladle lining using multi-response optimization techniques, grey relational analysis (GRA), and the technique for order preference by similarity to ideal solution (TOPSIS). A mixed-level orthogonal array $L_{32}$ ($4^9 \times 2^1$) was applied to the lining concept design, considering the material properties and lining thicknesses. FE modeling was performed to obtain the thermal and thermomechanical responses. Subsequently, GRA and TOPSIS were employed to convert the multiple responses to a single response and rank the lining configurations to select the best solution. The combination of optimal levels of factors and the percentage of factor contribution to the overall performance characteristic were obtained through the signal-to-noise (S/N) ratio and analysis of variance (ANOVA).

## 2. Methodology

### 2.1. Establishment of the Factor-Response dataset

The lining at the slag-line area shows the highest wear rate in the ladle and was selected for the study. Ten factors describing slag-line area lining were selected for the lining concept design. These factors (**Table 1**) were the thicknesses of the refractory linings and steel shell, thermal conductivity, and Young's modulus of the lining materials. The lining configurations were designed in a previous study[18] by applying a mixed-level orthogonal array $L_{32}$ ($4^9 \times 2^1$) with 9 four-level factors and a two-level factor for the steel ladle thickness. This reduced the total number of lining configurations from 524 288 to 32.

**Table 1.** Geometrical and material property factors of a steel ladle.[18]

| Impact factors | | Levels | | | | Label of factors |
|---|---|---|---|---|---|---|
| | | 1 | 2 | 3 | 4 | |
| Thickness [mm] | Working lining | 250 | 200 | 155 | 50 | A |
| | Permanent lining | 130 | 110 | 90 | 65 | B |
| | Insulation lining | 37.5 | 25 | 15 | 6 | C |
| | Steel shell | 30 | 20 | | | J |
| Thermal conductivity [$Wm^{-1} K^{-1}$] | Working lining | 9 | 8.5 | 7 | 3 | D |
| | Permanent lining | 9 | 5 | 3 | 2.2 | E |
| | Insulation lining | 1.35 | 0.5 | 0.35 | 0.15 | F |
| Young's modulus [GPa] | Working lining | 100 | 80 | 60 | 40 | G |
| | Permanent lining | 90 | 45 | 30 | 10 | H |
| | Insulation lining | 35 | 4 | 3 | 0.17 | I |

Thermal and thermomechanical responses were obtained through FE simulations considering the elastic material behavior using the commercial software ABAQUS. The responses were the end temperature and the maximum tensile stress at the cold end of the steel shell and the maximum compressive stress at the hot face of the working lining. **Figure 1** illustrates the simplified plane strain model representing a horizontal cut through the slag-line area in the upper part of the steel ladle.[18] The model was composed of a two-half brick working and permanent lining, an insulation layer, a fiberboard, and a steel shell. The circumferential expansion allowance between bricks was 0.4 mm. The model with two symmetrical halves was advantageous for the contact simulation. The simulated process included preheating of the hot face of the working lining for 20 h to 1100 °C, tapping the steel melt of 1600 °C into the ladle, refining for 95 min, and a 50 min idle period. The displacement of the linings was free in the radial direction and constrained in the circumferential direction under a symmetry condition. The heat transfer between the melt and the hot face of the working lining and the cold end of the steel shell and the atmosphere was defined by the temperature-dependent surface film condition function in ABAQUS. The heat flux crossed the interfaces between the lining materials. Radiation and convection were considered using a heat transfer coefficient.

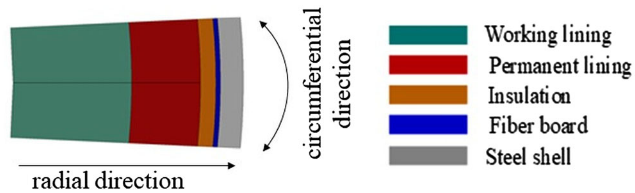


**Figure 1.** Plane strain model of the steel ladle slag zone lining.[18]

### 2.2. GRA

Deng proposed the grey system theory to address poor, incomplete, and uncertain information.[19] GRA[20] is a part of the grey system theory and has been successfully applied to solve multi-response optimization problems in several fields.[21–24] In the steelmaking industry, it has been used in the determination of high-correlation indexes with silicon content in a blast furnace,[25] evaluation of the influencing factors of heat transfer in a blast furnace hearth,[26] optimization of the flow control device in the tundish,[27] and determination of the key factors affecting the hot metal temperature in a blast furnace.[28]

The optimization procedure using GRA is shown in **Figure 2**. The calculation steps involved in GRA are as follows.

Step 1: Normalization of the values of the responses to the range [0,1] with the equation for "the-lower-the-better" characteristic (Equation (1))[29] as in this study lower temperatures and stresses are desired

$$y_{ij}^{*} = \frac{\max(y_{ij}) - y_{ij}}{\max(y_{ij}) - \min(y_{ij})} \tag{1}$$

where $y_{ij}^{*}$ is the normalized value of the jth response in the $i$th alternative, $y_{ij}$ is the value of the jth response in the $i$th alternative, and $\max(y_{ij})$ and $\min(y_{ij})$ are the maximum and minimum values of $y_{ij}$, respectively.

Step 2: Calculation of the grey relational coefficients (GRCs) using Equation (2)–(5)[29] is as follows.

$$\xi_{ij} = \frac{\Delta_{\min} + \varphi\Delta_{\max}}{\Delta_{ij}^{\circ} - \varphi\Delta_{\max}} \tag{2}$$

$$\Delta_{ij}^{\circ} = |y_j^{*\circ} - y_{ij}^{*}| \tag{3}$$

$$\Delta_{\max} = \max_{\forall i} \max_{\forall j} |y_j^{*\circ} - y_{ij}^{*}| \tag{4}$$

$$\Delta_{\min} = \min_{\forall i} \min_{\forall j} |y_j^{*\circ} - y_{ij}^{*}| \tag{5}$$

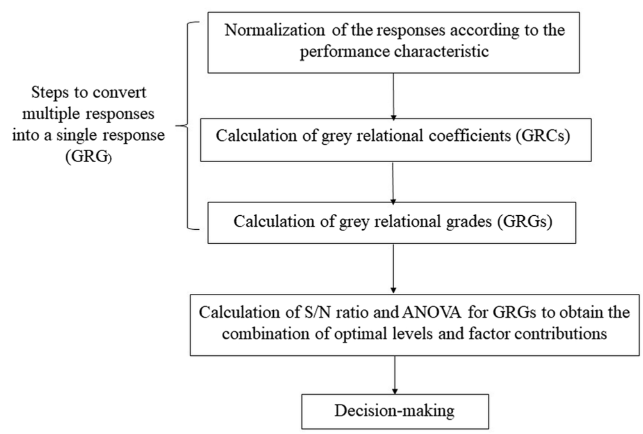


**Figure 2.** Flowchart of the optimization procedure using GRA.

where $\xi_{ij}$ is the GRC of the $j$th response in the $i$th alternative; $\varphi$ is the distinguishing coefficient, which is limited in the range $0 < \varphi < 1$[30] and generally $\varphi = 0.5$ is used;[31–34] $y_j^{*\circ}$ denotes the optimum value of the $j$th response; $\Delta_{ij}^{\circ}$ is the deviation value between $y_j^{*\circ}$ and $y_{ij}^{*}$, and $\Delta_{\max}$ and $\Delta_{\min}$ are the maximum and minimum values of $\Delta_{ij}^{\circ}$, respectively.

Step 3: Calculation of the grey relational grades (GRGs) using Equation (6) is as follows.[29]

$$\gamma_i = \sum_{j=1}^{n} w_j \xi_{ij} \tag{6}$$

where $\gamma_i$ is the GRG of the ith alternative, $w_j$ is the weight of the jth response, and $n$ is the number of responses.

In this study, the S/N ratio-based weight was determined and applied using the following equations.

$$\frac{S}{N} = -10 \log\left(\frac{1}{\mathrm{m}} \sum_{i=1}^{\mathrm{m}} y_i^2\right) \tag{7}$$

$$w_j = \frac{\sum_{i=1}^{\mathrm{p}} \mathrm{Delta}_{i,j}}{\sum_{j=1}^{n} \sum_{i=1}^{\mathrm{p}} \mathrm{Delta}_{i,j}} \tag{8}$$

where $m$ is the number of alternatives at one level of one factor, $y_i$ is the value of the ith alternative at one level of one factor, $p$ is the number of factors, $n$ is the number of responses, and $\mathrm{Delta}_{i,j}$ is the difference between the maximum and minimum S/N ratio of one factor.

### 2.3. TOPSIS

TOPSIS was pioneered by Hwang and Yoon in 1981.[35] It is a multi-objective decision-making approach that is widely used to determine the best alternative among an alternative set. Using TOPSIS, multiple responses are converted into a single response that is represented by the relative closeness to the ideal solution. The best alternative is the solution with the shortest and farthest Euclidean distance from the ideal and anti-ideal solutions, respectively. In the steelmaking industry, TOPSIS has been employed to select materials for furnaces,[16,36] access symbiotic technologies,[37] select green and sustainable suppliers,[38,39] adjust the burden surface in a blast furnace,[40] and solve the hot-rolling batch-scheduling problem.[41] The implementation procedure (**Figure 3**) of TOPSIS comprises several steps and is described as follows.

Step 1: Normalization of the responses using Equation (9) is calculated as follows.

$$\gamma_{ij} = \frac{y_{ij}}{\sqrt{\sum_{i=1}^{N} y_{ij}^2}} \tag{9}$$

where $\gamma_{ij}$ is the normalized value of the $j$th response in the ith alternative, $y_{ij}$ is the value of the jth response in the ith alternative, and $N$ is the number of alternatives.

Step 2: Calculation of the weighted normalized responses using Equation (10) is as follows

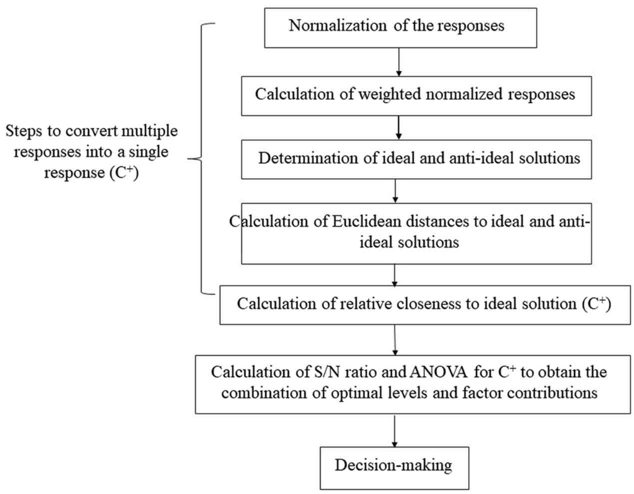


**Figure 3.** Flowchart of the optimization procedure using TOPSIS.

$$v_{ij} = \gamma_{ij} \times w_j \tag{10}$$

where $v_{ij}$ is the weighted normalized value of the jth response in the ith alternative, $w_j$ is the weight of the jth response, and $\sum_{i=1}^{n} w_j = 1$ is for a dataset with $n$ responses.

Step 3: Determination of the ideal ($A^+$) and anti-ideal ($A^-$) solutions for "the-lower-the-better" characteristic using Equation (11) and (12) is as follows.

$$A^+ = \{v_1^+, v_2^+, \ldots v_n^+\} = \min_{1 \le i \le N}(v_{ij}), \quad j = 1, 2, \ldots, n \tag{11}$$

$$A^- = \{v_1^-, v_2^-, \ldots v_n^-\} = \max_{1 \le i \le N}(v_{ij}), \quad j = 1, 2, \ldots, n \tag{12}$$

where $v_n^+$ and $v_n^-$ denote the ideal and anti-ideal solutions of the nth response, respectively; $N$ is the number of alternatives; $n$ is the number of responses.

Step 4: Calculation of Euclidean distances to the ideal ($A^+$) and anti-ideal ($A^-$) solutions using Equation (13) and (14) as follows.

$$D_i^+ = \sqrt{\sum_{j=1}^{n} (v_{ij} - v_j^+)^2} \tag{13}$$

$$D_i^- = \sqrt{\sum_{j=1}^{n} (v_{ij} - v_j^-)^2} \tag{14}$$

Step 5: Calculation of the relative closeness of each alternative to the ideal solution is as follows.

$$C_i^+ = \frac{D_i^-}{D_i^+ + D_i^-} \tag{15}$$

The relative closeness $C^+$ was used to rank the alternatives. A high $C^+$ value indicates a better performance and the best alternative was that with the highest $C^+$ value.

## 3. Results and Discussion

### 3.1. Optimization with GRA

#### 3.1.1. Best Solution

The values of all cases for each response were normalized using Equation (1). Subsequently, the GRCs for each response were determined using Equation (2)–(5) and a distinguishing coefficient of 0.5. Finally, the GRGs of all cases were obtained using Equation (6) considering the S/N ratio-based weights (computed using Equation (7) and (8)) which were 0.48, 0.28, and 0.24 for the temperature, tensile stress, and compressive stress, respectively. In this step, the multiple response problem was converted into a single-response (GRG) problem. The normalized values, the GRC of each response, and the GRG are provided in **Table 2**. The ranking of the lining configurations is shown in **Figure 4**. A higher GRG value indicates a better performance. Thus, the fourth case provides the best thermal and thermomechanical performance among all the lining configurations. The configuration of the fourth case is summarized in **Table 3**. The detailed thermal and thermomechanical performance of the fourth case is shown in **Figure 5**. The cold end temperature at the end of the idle time was 170 °C. The maximum compressive stress at the hot face and maximum tensile stress at the cold end during the simulation was 542 and 1111 MPa, respectively. The value ranges of all 32 cases (temperature [132, 434], compressive stress [423, 1025], and tensile stress [1110, 2279]) confirmed the good overall thermal and thermomechanical performance of the fourth case.

#### 3.1.2. The Combination of Optimal Levels

To obtain the combination of optimal levels, the S/N ratios were calculated for GRG. Because a higher GRG value indicates a better performance, Equation (16)[42] for the larger-the-better characteristic was employed to evaluate GRG. For each factor, the optimal level was that with the highest S/N ratio. As shown in **Figure 6**, the combination of optimal levels for GRG was A1B1C1D4E2F4G4H3I4J1

$$\frac{S}{N} = -10 \log\left(\frac{1}{\mathrm{m}} \sum_{i=1}^{\mathrm{m}} \frac{1}{\gamma_i^2}\right) \tag{16}$$

where $m$ is the number of alternatives at one level of one factor and $\gamma_i$ is the value of the ith alternative at one level of one factor.

#### 3.1.3. Factor Contribution

ANOVA, a statistical tool, was used to quantitatively assess the main factors affecting the GRGs obtained with a distinguishing coefficient of 0.5. The percentage contribution of each factor to GRG is shown in **Figure 7**. The results demonstrate that the factor G, Young's modulus of the working lining, which contributes 46.92% to the GRG, is the dominant factor. The following significant factors are the thermal conductivity of the working lining (D), the thickness of the insulation (C), the thickness of the working lining (A), and the thermal conductivity of the insulation (F). These top five factors contribute 89% of the total contribution

**Table 2.** Normalized responses, GRC, and GRG.

| Case number | Normalized responses | | | GRC | | | GRG |
|---|---|---|---|---|---|---|---|
| | Temperature | Tensile stress | Compressive stress | Temperature | Tensile stress | Compressive stress | |
| 1 | 0.5693 | 0.4038 | 0.0415 | 0.4676 | 0.5532 | 0.9233 | 0.4679 |
| 2 | 0.6673 | 0.4269 | 0.2691 | 0.4283 | 0.5395 | 0.6501 | 0.5162 |
| 3 | 0.6861 | 0.5808 | 0.5266 | 0.4216 | 0.4626 | 0.4871 | 0.5705 |
| 4 | 0.8781 | 0.9991 | 0.7857 | 0.3628 | 0.3335 | 0.3889 | 0.8332 |
| 5 | 0.6931 | 0.4132 | 0.1063 | 0.4191 | 0.5475 | 0.8247 | 0.5124 |
| 6 | 0.3778 | 0.5595 | 0.3256 | 0.5696 | 0.4719 | 0.6056 | 0.4648 |
| 7 | 0.7008 | 0.4919 | 0.5465 | 0.4164 | 0.5041 | 0.4778 | 0.5651 |
| 8 | 0.7746 | 1.0000 | 0.7841 | 0.3923 | 0.3333 | 0.3894 | 0.7781 |
| 9 | 0.6354 | 0.5227 | 0.4136 | 0.4404 | 0.4889 | 0.5473 | 0.5313 |
| 10 | 0.8894 | 0.0000 | 0.0515 | 0.3599 | 1.0000 | 0.9066 | 0.5695 |
| 11 | 0.3361 | 0.8854 | 0.8837 | 0.5980 | 0.3609 | 0.3613 | 0.6285 |
| 12 | 0.6325 | 0.8777 | 0.4684 | 0.4415 | 0.3629 | 0.5163 | 0.6176 |
| 13 | 0.0213 | 0.7853 | 0.3023 | 0.9591 | 0.3890 | 0.6232 | 0.4580 |
| 14 | 0.1979 | 0.7032 | 0.0000 | 0.7165 | 0.4156 | 1.0000 | 0.4397 |
| 15 | 0.6419 | 0.2344 | 0.9601 | 0.4379 | 0.6808 | 0.3424 | 0.6130 |
| 16 | 0.6878 | 0.9683 | 0.5415 | 0.4210 | 0.3405 | 0.4801 | 0.6836 |
| 17 | 0.7365 | 0.4611 | 0.9302 | 0.4044 | 0.5202 | 0.3496 | 0.6600 |
| 18 | 0.5172 | 0.4679 | 0.6910 | 0.4916 | 0.5166 | 0.4198 | 0.5283 |
| 19 | 1.0000 | 0.0950 | 0.3339 | 0.3333 | 0.8404 | 0.5996 | 0.6829 |
| 20 | 0.9008 | 0.3388 | 0.0615 | 0.3569 | 0.5961 | 0.8905 | 0.6047 |
| 21 | 0.7915 | 0.3661 | 0.9385 | 0.3871 | 0.5773 | 0.3476 | 0.6763 |
| 22 | 0.9356 | 0.1078 | 0.6379 | 0.3483 | 0.8227 | 0.4394 | 0.6654 |
| 23 | 0.2501 | 0.5654 | 0.5133 | 0.6665 | 0.4693 | 0.4934 | 0.4634 |
| 24 | 0.6714 | 0.4234 | 0.1246 | 0.4269 | 0.5415 | 0.8005 | 0.5069 |
| 25 | 0.2978 | 0.3704 | 0.7093 | 0.6267 | 0.5744 | 0.4135 | 0.4754 |
| 26 | 0.3193 | 0.4919 | 0.9734 | 0.6103 | 0.5041 | 0.3393 | 0.5702 |
| 27 | 0.6596 | 0.3550 | 0.2741 | 0.4312 | 0.5848 | 0.6459 | 0.5058 |
| 28 | 0.7912 | 0.4671 | 0.3189 | 0.3872 | 0.5170 | 0.6105 | 0.5758 |
| 29 | 0.0000 | 0.7802 | 0.6794 | 1.0000 | 0.3906 | 0.4239 | 0.5005 |
| 30 | 0.3299 | 0.7288 | 1.0000 | 0.6025 | 0.4069 | 0.3333 | 0.6267 |
| 31 | 0.3060 | 0.3464 | 0.2276 | 0.6204 | 0.5907 | 0.6872 | 0.4166 |
| 32 | 0.6767 | 0.3533 | 0.3173 | 0.4249 | 0.5860 | 0.6118 | 0.5151 |

and are related to the thicknesses and material properties of the working lining and insulation.

### 3.2. Optimization using TOPSIS

#### *3.2.1. Best Solution*

The values of the responses were normalized using Equation (9). The weighted normalized responses were determined using Equation (10), considering the S/N ratio-based weights, which were 0.48, 0.28, and 0.24 for the temperature, tensile stress, and compressive stress, respectively. After the normalization, the ideal ($A^+$) and anti-ideal ($A^-$) solutions were determined using Equation (11) and (12). The Euclidean distances from the alternatives to the ideal ($D_i^+$) and anti-ideal ($D_i^-$) solutions were computed using Equation (13) and (14). The relative closeness of the alternatives to the ideal solution ($C_i^+$) is computed using Equation (15). The normalized responses, weighted normalized responses, $D_i^+$, $D_i^-$, and $C_i^+$ are provided in **Table 4**. The alternative with the highest relative closeness, $C^+$, is considered the best solution. According to the ranking of relative closeness (**Figure 8**), the fourth lining configuration was the best among the 32 cases.

#### *3.2.2. The Combination of Optimal Levels*

Equation (16) for the larger-the-better characteristic was used to compute the S/N ratios for relative closeness ($C^+$). The optimal

steel research international
www.steel-research.de

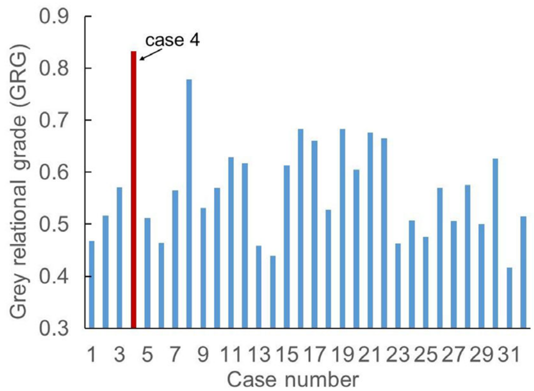


**Figure 4.** GRG for all cases.

**Table 3.** The configuration of the fourth case.

| | Thickness [mm] | Thermal conductivity [W m$^{-1}$ K$^{-1}$] | Young's modulus [GPa] |
|---|---|---|---|
| Working lining | 250 | 3 | 40 |
| Permanent lining | 65 | 2.2 | 10 |
| Insulation | 6 | 0.15 | 0.17 |
| Steel shell | 30 | | |

level of one factor was the level with the highest S/N ratio among all levels. The S/N ratio for $C^+$ is shown in **Figure 9**. The combination of optimal levels was A1B1C1D4E3F4G4H1I4J1.

### 3.2.3. Factor Contribution

ANOVA was performed to evaluate the significance of the factors to the relative closeness $C^+$. The percentage contributions of the factors to $C^+$ are shown in **Figure 10**. Factor A, the thickness of the working lining, was the most significant factor for $C^+$. It contributed 26.68% to $C^+$. The second most important factor was factor D, the thermal conductivity of the working lining, with a contribution of 23.06%. The subsequent significant factors

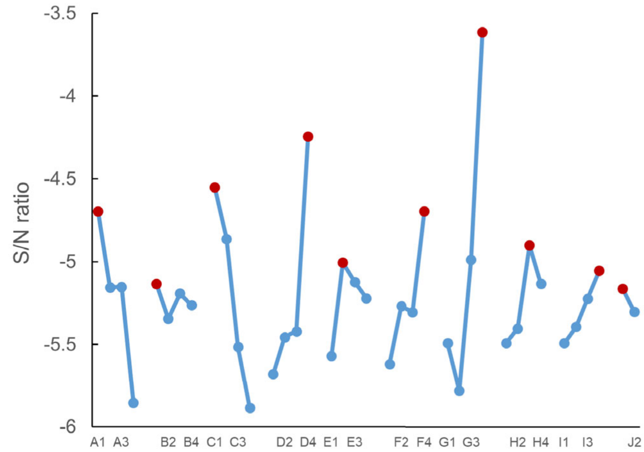


**Figure 6.** S/N ratio for GRG.

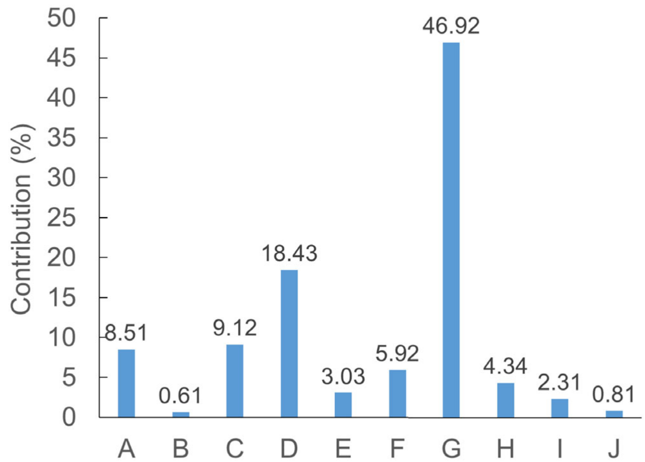


**Figure 7.** Factor contribution to GRG.

were the thickness of the insulation (C), thermal conductivity of the insulation (F), and Young's modulus of the working lining (G). The contributions of factors C, F, and G to $C^+$ were

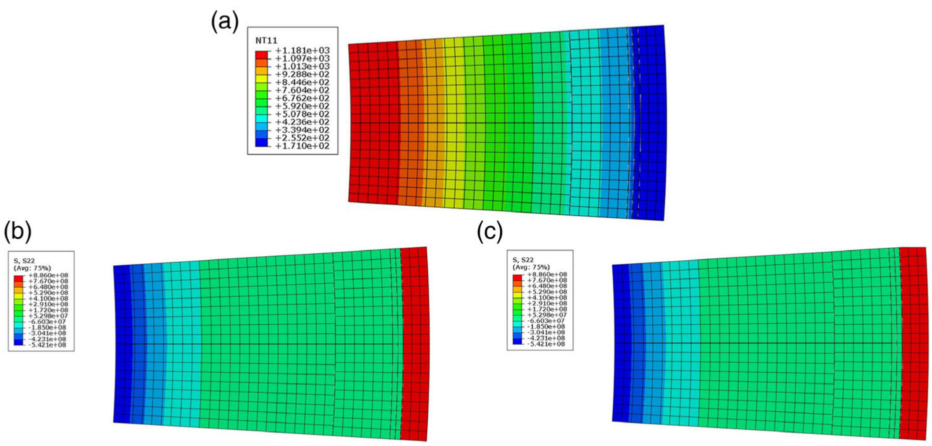


**Figure 5.** The thermal and thermomechanical performance of the fourth case: a) temperature distribution at the end of the idle time, b) maximum compressive stress at the hot face, c) maximum tensile stress at the cold end.

**Table 4.** Normalized responses, weighted normalized responses, $D_i^+$, $D_i^-$, and $C_i^+$.

| Case number | Normalized responses | | | Weighted normalized responses | | | $D_i^+$ | $D_i^-$ | $C_i^+$ |
|---|---|---|---|---|---|---|---|---|---|
| | Temperature | Tensile stress | Compressive stress | Temperature | Tensile stress | Compressive stress | | | |
| 1 | 0.1714 | 0.1879 | 0.2351 | 0.0823 | 0.0526 | 0.0564 | 0.0561 | 0.0558 | 0.4988 |
| 2 | 0.1521 | 0.1851 | 0.2029 | 0.0730 | 0.0518 | 0.0487 | 0.0447 | 0.0657 | 0.5951 |
| 3 | 0.1484 | 0.1664 | 0.1664 | 0.0712 | 0.0466 | 0.0399 | 0.0368 | 0.0704 | 0.6570 |
| 4 | 0.1104 | 0.1155 | 0.1298 | 0.0530 | 0.0324 | 0.0311 | 0.0137 | 0.0939 | 0.8729 |
| 5 | 0.1470 | 0.1868 | 0.2259 | 0.0705 | 0.0523 | 0.0542 | 0.0466 | 0.0674 | 0.5914 |
| 6 | 0.2093 | 0.1690 | 0.1949 | 0.1005 | 0.0473 | 0.0468 | 0.0651 | 0.0421 | 0.3926 |
| 7 | 0.1454 | 0.1772 | 0.1636 | 0.0698 | 0.0496 | 0.0393 | 0.0367 | 0.0711 | 0.6598 |
| 8 | 0.1308 | 0.1154 | 0.1300 | 0.0628 | 0.0323 | 0.0312 | 0.0226 | 0.0853 | 0.7904 |
| 9 | 0.1584 | 0.1735 | 0.1824 | 0.0760 | 0.0486 | 0.0438 | 0.0431 | 0.0645 | 0.5992 |
| 10 | 0.1081 | 0.2370 | 0.2337 | 0.0519 | 0.0664 | 0.0561 | 0.0480 | 0.0845 | 0.6376 |
| 11 | 0.2176 | 0.1294 | 0.1159 | 0.1045 | 0.0362 | 0.0278 | 0.0633 | 0.0532 | 0.4566 |
| 12 | 0.1590 | 0.1303 | 0.1747 | 0.0763 | 0.0365 | 0.0419 | 0.0395 | 0.0689 | 0.6356 |
| 13 | 0.2799 | 0.1415 | 0.1982 | 0.1343 | 0.0396 | 0.0476 | 0.0962 | 0.0287 | 0.2298 |
| 14 | 0.2450 | 0.1515 | 0.2410 | 0.1176 | 0.0424 | 0.0578 | 0.0840 | 0.0304 | 0.2659 |
| 15 | 0.1571 | 0.2085 | 0.1051 | 0.0754 | 0.0584 | 0.0252 | 0.0429 | 0.0696 | 0.6188 |
| 16 | 0.1480 | 0.1193 | 0.1643 | 0.0710 | 0.0334 | 0.0394 | 0.0335 | 0.0754 | 0.6924 |
| 17 | 0.1384 | 0.1810 | 0.1093 | 0.0664 | 0.0507 | 0.0262 | 0.0311 | 0.0783 | 0.7157 |
| 18 | 0.1818 | 0.1801 | 0.1432 | 0.0872 | 0.0504 | 0.0344 | 0.0504 | 0.0567 | 0.5295 |
| 19 | 0.0862 | 0.2255 | 0.1937 | 0.0414 | 0.0631 | 0.0465 | 0.0382 | 0.0957 | 0.7146 |
| 20 | 0.1059 | 0.1958 | 0.2323 | 0.0508 | 0.0548 | 0.0557 | 0.0401 | 0.0864 | 0.6826 |
| 21 | 0.1275 | 0.1925 | 0.1081 | 0.0612 | 0.0539 | 0.0260 | 0.0294 | 0.0826 | 0.7378 |
| 22 | 0.0990 | 0.2239 | 0.1507 | 0.0475 | 0.0627 | 0.0362 | 0.0333 | 0.0915 | 0.7330 |
| 23 | 0.2346 | 0.1683 | 0.1683 | 0.1126 | 0.0471 | 0.0404 | 0.0746 | 0.0352 | 0.3206 |
| 24 | 0.1513 | 0.1855 | 0.2233 | 0.0726 | 0.0519 | 0.0536 | 0.0474 | 0.0655 | 0.5804 |
| 25 | 0.2252 | 0.1920 | 0.1406 | 0.1081 | 0.0538 | 0.0337 | 0.0707 | 0.0392 | 0.3568 |
| 26 | 0.2209 | 0.1772 | 0.1032 | 0.1060 | 0.0496 | 0.0248 | 0.0669 | 0.0479 | 0.4171 |
| 27 | 0.1536 | 0.1939 | 0.2022 | 0.0737 | 0.0543 | 0.0485 | 0.0462 | 0.0645 | 0.5825 |
| 28 | 0.1275 | 0.1802 | 0.1958 | 0.0612 | 0.0505 | 0.0470 | 0.0355 | 0.0776 | 0.6863 |
| 29 | 0.2841 | 0.1422 | 0.1448 | 0.1364 | 0.0398 | 0.0348 | 0.0959 | 0.0352 | 0.2684 |
| 30 | 0.2188 | 0.1484 | 0.0994 | 0.1050 | 0.0416 | 0.0239 | 0.0643 | 0.0525 | 0.4492 |
| 31 | 0.2236 | 0.1949 | 0.2088 | 0.1073 | 0.0546 | 0.0501 | 0.0744 | 0.0323 | 0.3029 |
| 32 | 0.1502 | 0.1941 | 0.1961 | 0.0721 | 0.0543 | 0.0471 | 0.0443 | 0.0663 | 0.5991 |

16.77%, 12.38%, and 8.22%, respectively. The total contribution of the top five factors to $C^+$ was 87%.

### 3.3. Comparison of GRA and TOPSIS

The multi-response optimization problem was converted into a single-response optimization problem using GRA and TOPSIS. GRA and TOPSIS results indicated that the fourth lining configuration was the best solution among the 32 alternatives. In comparison with the optimal level combination obtained from GRA (A1B1C1D4E2F4G4H3I4J1), the TOPSIS results (A1B1C1D4E3F4G4H1I4J1) demonstrated that the optimal levels of factor E (thermal conductivity of the permanent lining) and factor H (Young's modulus of the permanent lining) differed from those of GRA. The factor contributions from GRA and TOPSIS results indicated that these two factors were not the top significant factors. Therefore, the combination of optimal levels for significant factors (A1B1C1D4F4G4I4J1) was the same as that of GRA and TOPSIS. The top five most significant factors for GRG and $C^+$ were the same. The sum of the percentage contributions of the top five factors to GRG (89%) and $C^+$(87%) was similar.

### 3.4. Comparison of GRA and TOPSIS with the conventional Taguchi method

The conventional Taguchi method is a single-response optimization technique. In this case, the three responses must be

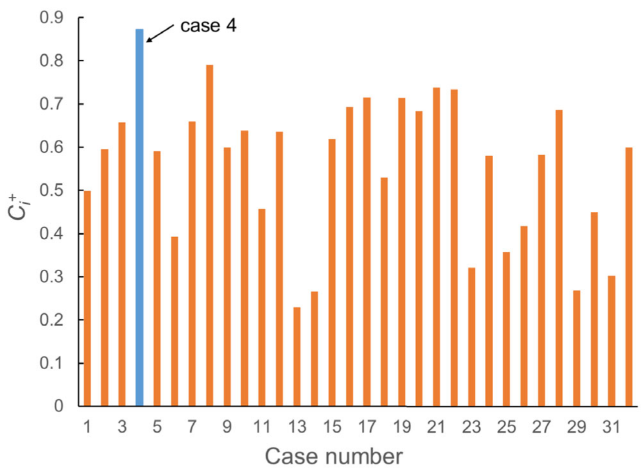


**Figure 8.** Relative closeness to $C_i^+$.

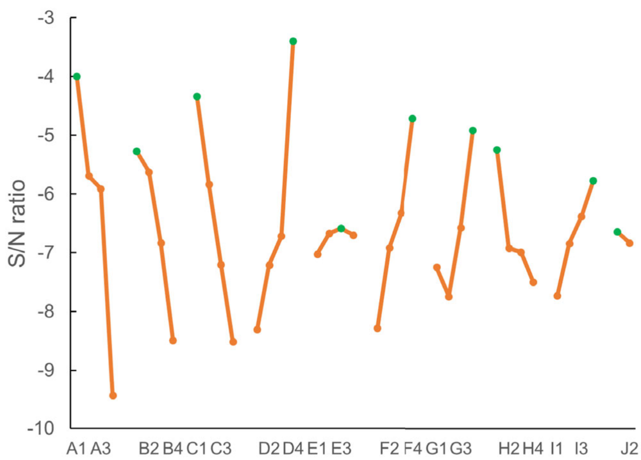


**Figure 9.** S/N ratio for the relative closeness to $C^+$.

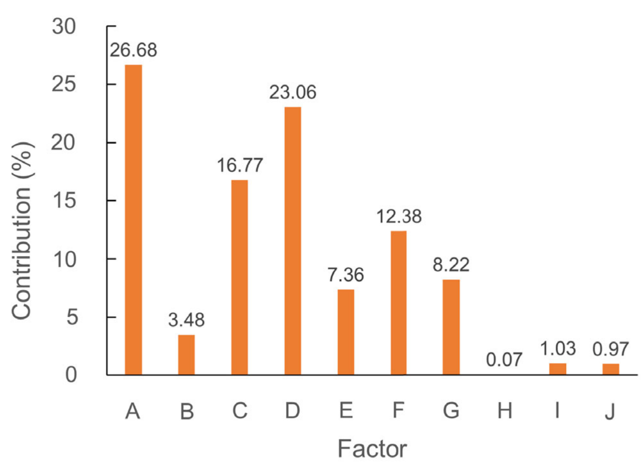


**Figure 10.** Factor contribution to $C^+$.

individually optimized. The Taguchi results[18] revealed that some factors had a contradictory influence on different responses, as summarized in **Table 5**. For instance, larger thicknesses of the working lining (A), insulation (C), and insulation with lower thermal conductivity (factor F) result in lower temperatures at the cold end of the steel shell; however, they cause higher tensile stresses at the steel shell. Similarly, the working lining with a larger Young's modulus offers lower compressive stresses at the hot face of the working lining but results in higher tensile stresses at the steel shell. Decision-makers can prioritize larger thicknesses of the working lining (A) and insulation (C) and lower the Young's modulus of the working lining (G), as these factors contribute significantly to one response than the other. For instance, factor A contributes 31% to the end temperature and 5% to the tensile stress. However, factor F is a significant factor for the two responses, which contributes 20% to the end temperature and 24% to the tensile stress. Therefore, it is difficult to make a trade-off and more quantitative information about the significance of the factors is desired.

Multiple responses can be optimized simultaneously using GRA and TOPSIS. Both techniques can convert multiple responses into a single response. After employing the S/N ratio and ANOVA, the optimal levels and factor contributions were obtained. With GRA and TOPSIS, the difficulties in handling factors that have a contradictory influence on different responses are solved, and the quantitative factor contribution for multiple responses is provided for decision-makers. For instance, the optimal levels of factors A, C, and G are the same with those obtained using the Taguchi method. For factor F, which is difficult to handle using the Taguchi method, quantitative information was provided by the GRA and TOPSIS results.

## 4. Conclusion

GRA and TOPSIS were successfully applied to simultaneously optimize the thermal and thermomechanical behavior of a steel ladle lining considering the influence of lining thicknesses and material properties. GRA and TOPSIS results after applying a distinguishing coefficient of 0.5 in GRA and the S/N ratio-based weight in both methods indicated the same best solution (the fourth lining configuration), the same optimal levels for the significant factors, and the same top five factors with a total contribution similar to the overall performance characteristic.

GRA and TOPSIS can optimize multiple responses simultaneously and overcome the disadvantages of the conventional Taguchi method, e.g., expert experience is required to inform decisions when a factor has a contradictory influence on different responses. The ladle lining is a complex system and the final optimized solution should also take the situation into account. For instance, the bricks that are available and whether their properties are close to the optimal values. Therefore, the multi-response optimization of linings considering commercial refractory materials and irreversible material behavior, such as creep, tensile failure, and shear failure, is of interest for future research.

**Table 5.** Comparison of conventional Taguchi method, GRA, and TOPSIS.

| Methods | Targets | Factor A | | Factor C | | Factor F | | Factor G | |
|---|---|---|---|---|---|---|---|---|---|
| | | OL* | CO* [%] | OL | CO [%] | OL | CO [%] | OL | CO [%] |
| Conventional Taguchi method | $T\downarrow$ | 1 (250 mm) | 31 | 1 (37.5 mm) | 20 | 4 (0.15 $\text{W m}^{-1}\text{K}^{-1}$) | 20 | 1 (100 GPa) | 1 |
| | $\sigma_{\text{Ten}}\downarrow$ | 4 (50 mm) | 5 | 4 (6 mm) | 7 | 1 (1.35 $\text{W m}^{-1}\text{K}^{-1}$) | 24 | 4 (40 GPa) | 17 |
| | $\sigma_{\text{Comp}}\downarrow$ | | | | | | | 4 (40 GPa) | 93 |
| GRA | GRG $\uparrow$ | 1 (250 mm) | 8.51 | 1 (37.5 mm) | 9.12 | 4 (0.15 $\text{W m}^{-1}\text{K}^{-1}$) | 5.92 | 4 (40 GPa) | 46.92 |
| TOPSIS | $C_i^+\uparrow$ | 1 (250 mm) | 26.68 | 1 (37.5 mm) | 16.77 | 4 (0.15 $\text{W m}^{-1}\text{K}^{-1}$) | 12.38 | 4 (40 GPa) | 8.22 |

OL*: Optimal Levels; CO*: Contribution.

## Acknowledgements

The Competence Center for Excellent Technologies research programme in "Advanced Metallurgical and Environmental Process Development" (K1-MET) is supported by the Austrian Competence Centre Programme COMET (Competence Center for Excellent Technologies) with funds from the Federal Ministry for Transport, Innovation and Technology, the Federal Ministry of Economy, the provinces of Upper Austria and Styria, the Styrian Business Promotion Agency, and the Tyrolian Future Foundation.

## Conflict of Interest

The authors declare no conflict of interest.

## Data Availability Statement

The data that support the findings of this study are available from the corresponding author upon reasonable request.

## Keywords

GRA, lining optimizations, steel ladles, thermal and thermomechanical behaviors, TOPSIS

Received: May 16, 2022
Revised: September 16, 2022
Published online:

[1] T. Vert, *Refractory Material Selection for Steelmaking*, Wiley, Hoboken, NJ **2016**.
[2] D. H. Hubble, R. O. Russell, H. L. Vernon, R. J. Marr, *Steelmaking and Refining Volume*, The AISE Steel Foundation, PA **1998**.
[3] D. Gruber, T. Auer, H. Harmuth, J. Rotsch, in *STEELSIM2007*, Austria **2007**.
[4] D. Gruber, H. Harmuth, *Steel Res. Int.* **2014**, *85*, 512.
[5] D. Gruber, H. Harmuth, *Steel Res. Int.* **2008**, *79*, 913.
[6] S. Jin, D. G. T. Auer, H. Harmuth, M. H. Frechette, Y. Li, *Int. Ceram. Rev.* **2012**, 37.
[7] H. Zhang, P. Zhou, F. Yuan, *Energy* **2021**, *214*, 118896.
[8] G. Li, J. Liu, G. Jiang, H. Liu, *Adv. Mech. Eng.* **2015**, *7*, https://doi.org/10.1177/1687814015575988.
[9] M. F. Santos, M. H. Moreira, M. G. G. Campos, P. I. B. G. B. Pelissari, R. A. Angelico, E. Sako, S. Sinnema, V. C. Pandolfelli, *Ceram. Int.* **2018**, *44*, 12831.
[10] M. G. G. Campos, M. F. D. Santos, M. H. Moreira, R. A. Angelico, E. Y. Sako, V. C. Pandolfelli, *Int. J. Ceram. Eng. Sci.* **2020**, *2*, 113.
[11] M. F. Santos, M. H. Moreira, M. G. G. Campos, R. A. Angelico, E. Y. Sako, V. P. S. Ramos, D. F. Galesi, V. C. Pandolfelli, *Refract. Worldforum* **2020**, *12*, 36.
[12] M. Ali, T. Sayet, A. Gasser, E. Blond, *Ceramics* **2020**, *3*, 171.
[13] M. Ali, T. Sayet, A. Gasser, E. Blone, *Int. J. Mech. Sci.* **2021**, *196*, 106275.
[14] A. Gasser, L. Chen, F. Genty, J. L. Daniel, E. Blond, K. Andreev, S. Sinnema, in *UNITECR2013*, Canada **2013**.
[15] G. Li, J. Liu, G. Jiang, J. Kong, L. Xie, Z. Li, *Int. J. Online Biomed. Eng.* **2013**, *9*, 5.
[16] D. P. Santos, P. I. B. G. B. Pelissari, B. S. Oliveira, D. R. Leiva, R. F. Mello, V. C. Pandolfelli, *Ceram. Int.* **2020**, *46*, 4113.
[17] U. Asgher, J. A. Ruiz, R. Ahmad, O. M. Valdes, Y. Ayaz, S. Ali, *Advances in Neuroergonomics and Cognitive Engineering (AHFE 2019)*, Springer, USA **2019**.
[18] A. Hou, S. Jin, D. Gruber, H. Harmuth, *JOM* **2018**, *70*, 249.
[19] J. Deng, *Syst. Control Lett.* **1982**, *5*, 288.
[20] J. Deng, *Social Sci. China* **1984**, *6*, 47.
[21] A. Kazemlan, A. S. A. Parcheforosh, T. Ma, *Sol. Energy* **2021**, *215*, 492.
[22] S. Senthilkumar, A. Karthick, R. M. Adavan, A. A. M. Moshi, S. R. S. Bharathi, S. Saroja, C. S. Dhanalakshmi, *Fuel* **2021**, *288*, 119629.
[23] X. Ye, Y. Kang, B. Chen, S. Deng, Z. Yan, K. Zhong, *Build. Environ.* **2021**, *188*, 107431.
[24] E. Bulut, E. I. Albak, G. Sevilgen, F. Ozturk, *Case Stud. Therm. Eng.* **2021**, *28*, 101452.
[25] W. Chen, F. Kong, B. Wang, Y. Li, *Ironmaking Steelmaking* **2019**, *46*, 974.
[26] R. Zhu, P. Zhou, J. L. C. Zhou, *Ironmak. Steelmak.* **2018**, *45*, 899.
[27] D. Sheng, *Metals* **2020**, *10*, 1539.
[28] Y. Yue, A. Dong, H. Zhao, H. Wang, in *Int. Conf. Mechatronics and Automation*, China **2016**.
[29] Y. Kuo, T. Yang, G. Huang, *Eng. Optim.* **2008**, *40*, 517.
[30] J. Deng, *J. Grey Syst.* **1989**, *1*, 1.
[31] A. H. Bademlioglu, A. S. Canbolat, O. Kaynakli, *Renewable Sustainable Energy Rev.* **2020**, *117*, 109483.
[32] A. S. Canbolat, N. A. O. K. A. H. Bademlioglu, *J. Cleaner Prod.* **2019**, *229*, 874.
[33] A. Acir, M. E. Canli, I. Ata, R. Cakiroglu, *Appl. Therm. Eng.* **2017**, *122*, 330.
[34] T. Singh, A. Patnaik, R. Chauhan, *Mater. Des.* **2016**, *89*, 1335.
[35] C. L. Hwang, K. Yoon, *Lecture Notes in Economics and Mathematical Systems*, Springer, Germany **1981**.
[36] A. Rayhanizadeh, N. Towhidi, Y. S. S. Ebrahimnejad, *Eng. Res. Express* **2020**, *2*, 025009.

[37] Y. Wang, Z. Wen, H. Li, *J. Cleaner Prod.* **2020**, *260*, 120900.
[38] S. Kumar, A. G. Barman, *Soft Comput.* **2021**, *25*, 6505.
[39] A. Azimifard, S. H. Moosavirad, S. Ariafar, *Resour. Policy* **2018**, *57*, 30.
[40] Y. Li, H. Li, J. Zhang, S. Zhang, Y. Yin, *IEEE Access* **2020**, *8*, 35712.
[41] S. Jia, J. Yi, G. Yang, B. Du, J. Zhu, *Int. J. Prod. Res.* **2013**, *51*, 667.
[42] R. K. Roy, *A Primer on the Taguchi Method*, 2nd ed., Society of Manufacturing Engineers, USA **2010**.